

Supramolecular Architectures of Meloxicam Carboxylic Acid Cocrystals, a Crystal Engineering Case Study

Miranda L. Cheney,^{†,‡} David R. Weyna,^{†,‡} Ning Shan,^{*,†} Mazen Hanna,[†] Lukasz Wojtas,[‡] and Michael J. Zaworotko^{*,‡}

[†]Thar Pharmaceuticals Inc., 3802 Spectrum Boulevard, Suite 120, Tampa, Florida 33612, and

[‡]Department of Chemistry, University of South Florida, 4202 East Fowler Avenue, CHE205, Tampa, Florida 33620

Received April 17, 2010; Revised Manuscript Received August 2, 2010

ABSTRACT: Meloxicam is a nonsteroidal anti-inflammatory drug with low aqueous solubility and high permeability prescribed for indications of arthritis, primary dysmenorrhea, fever, and pain. In this contribution, we apply crystal engineering and the supramolecular synthon approach to prepare novel meloxicam cocrystal forms with various pharmaceutically acceptable or toxicologically qualified carboxylic acids. As a result, 19 pharmaceutical cocrystals including one cocrystal of a salt are synthesized by solid-state and solution methods. All resulting cocrystals are characterized by X-ray diffraction, infrared, and thermal analyses. In particular, crystal structures of six meloxicam cocrystals are determined and reported, namely, meloxicam · 1-hydroxy-2-naphthoic acid cocrystal (**1**), meloxicam · glutaric acid cocrystal (**2**), meloxicam · L-malic acid cocrystal of a salt (**3**), meloxicam · salicylic acid cocrystal form III (**4**), meloxicam · fumaric acid cocrystal (**5**), and meloxicam · succinic acid cocrystal (**6**). The supramolecular assembly of each cocrystal is analyzed and discussed. It is observed that the meloxicam dimer is robust since this motif is observed in five out of six meloxicam cocrystal structures that have been determined. As part of the continuous development, the resulting meloxicam cocrystal forms will be further investigated to explore improved physicochemical and pharmacological properties.

1. Introduction

Crystal form selection for oral delivery of active pharmaceutical ingredients (APIs) remains a high priority for the pharmaceutical industry.¹ In general, pharmaceutical crystal forms are preferred by developers and regulatory authorities, because crystallization tends to afford highly pure products that are superior with respect to reproducibility and scalability.¹ Moreover, a unique crystalline form may exhibit distinctive physicochemical properties and could in turn affect the dissolution, manufacturing, physical stability, permeability, and oral bioavailability of an API.^{2,3} Thus, it is apparent that selection of an appropriate crystal form for downstream development and processing is of primary importance in pharmaceutical development.⁴

A typical crystal form selection process comprises two stages of development after a target API molecule has been selected: discover as many pharmaceutical crystal forms as possible; then examine the physicochemical properties of the newly discovered crystal forms. At the stage of crystal form discovery, two primary approaches are used. The more straightforward approach is largely based on trial-and-error (e.g., high-throughput crystal form screening) and has been implemented to discover crystal forms including, but not limited to, salts,³ hydrates,⁵ solvates,⁶ and, more recently, cocrystals.^{7,8} The alternative approach for crystal form discovery is the supramolecular synthon approach,⁹ which recognizes supramolecular synthons¹⁰ as a design tool and can be more selective, time-efficient, and cost-effective. The supramolecular synthon approach uses crystal engineering¹¹ to carefully analyze the relevant supramolecular arrangements that an API might

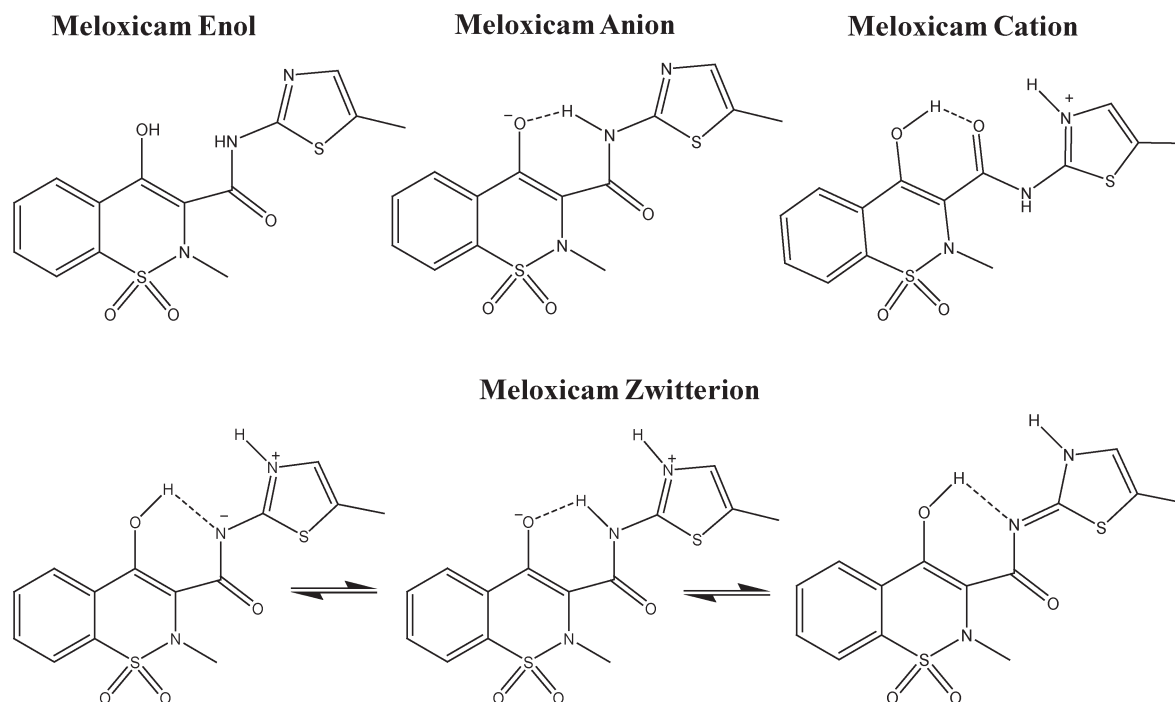
exhibit by utilizing the Cambridge Structural Database (CSD)¹² and effectively prioritizes all possible guest molecules for crystal form screening of drugs. Such an approach can be generally effective^{11b,d–i} but has found particular success in generating pharmaceutical cocrystals.^{9,13}

Pharmaceutical cocrystals are defined as multiple component crystals in which at least one component is molecular and a solid at room temperature (the coformer) and forms a supramolecular synthon with a molecular or ionic API.¹⁴ A given API may form cocrystals with numerous pharmaceutically acceptable or toxicologically qualified materials, and these cocrystals could exhibit enhanced solubility,^{9,15,16} stability to hydration, or compressibility.¹⁷ Therefore, pharmaceutical cocrystals represent an opportunity to diversify the number of crystal forms of a given API and in turn fine-tune or even customize its physicochemical properties without the need for chemical (covalent) modification. In addition, the supramolecular synthon approach can be implemented by various cocrystal preparative methods such as solution, slurry, grinding, or melt.^{18,19} Numerous APIs that exhibit undesirable solubility or stability and possess multiple hydrogen-bonding sites have been (or potentially can be) studied in the context of cocrystallization.^{15,20} As one of these potential APIs, meloxicam is identified and is of interest for cocrystallization.

Meloxicam, 4-hydroxy-2-methyl-*N*-(5-methyl-2-thiazolyl)-2*H*-1,2-benzothiazine-3-carboxamide-1,1-dioxide, is a nonsteroidal anti-inflammatory drug (NSAID) and an antipyretic drug used for indications of rheumatoid and osteoarthritis,²¹ postoperative pain,²² and fever.²³ Meloxicam is effective in relieving various types of pain and causes fewer side effects than other NSAIDs.²⁴ Compared with other drugs in the same class such as piroxicam, meloxicam is preferred due to its ability to selectively inhibit cyclooxygenase-2 (COX-2).²⁵ Originally developed by Boehringer Ingelheim, meloxicam is

*To whom correspondence should be addressed. E-mail addresses: nshan@tharpharma.com (N. Shan); xtal@usf.edu (M. J. Zaworotko).

Scheme 1. Enolic, Anionic, Cationic, and Zwitterionic Forms of Meloxicam



marketed in Europe under the brand names Melox or Recoxa and in the U.S. as Mobic. Meloxicam is available as an oral tablet (7.5 or 15 mg dose) and as an oral suspension (7.5 mg/5 mL dose).

Meloxicam is a yellow solid that is practically insoluble in water (0.012 mg/mL, 25 °C)²⁶ and is considered a Class II drug (i.e., a low-solubility and high-permeability drug) by the Biopharmaceutics Classification System (BCS).²⁷ Meloxicam is very slightly soluble in various organic solvents²⁶ and has variable aqueous solubility related to its pH-dependent ionization states. Under acidic conditions, meloxicam is present in its cationic form, while in basic solutions it is present in its anionic form. When the molecule is neutral in charge, meloxicam will either be in its zwitterionic or enolic form, depending on the polarity of the solvent.^{28,29} The different ionization states of meloxicam are shown in Scheme 1.

Due to its low solubility under acidic and neutral conditions, the T_{\max} (time to reach maximum concentration) of meloxicam in the human body is typically 4–6 hours, while it can take more than 2 hours for the drug to reach its therapeutic concentration in humans.³⁰ The slow onset of meloxicam prevents meloxicam from its potential application for the relief of mild or medium level acute pain. To accelerate its onset of action, various complexes of meloxicam have been prepared and evaluated with respect to aqueous solubility, resulting in cyclodextrin inclusion complexes,³¹ various solvates,²⁶ ethanolamine,³² ammonium, and sulfate salts,²⁸ or metal complexes with potassium and calcium.³³ Preparation of polymorphic crystal forms of meloxicam²⁹ has also been attempted to improve its dissolution profile.³⁴ Five polymorphic forms of meloxicam have been reported in the literature.²⁹ The stability and potential for solid-phase interconversion between various meloxicam polymorphic forms has not been investigated.³⁵ Despite all the efforts that have been taken, a faster onset dosage form for oral administration of meloxicam remains unknown to date. Only very recently did Myz et al.³⁶ report the preparation of two pharmaceutical cocrystals employing maleic acid and succinic

acid. Interestingly, pharmaceutical cocrystals of piroxicam, an API with a similar molecular structure to meloxicam (i.e., piroxicam possesses a pyridyl group rather than a thiazole group), have been reported and are used as a reference for this study.³⁷ Clearly, pharmaceutical cocrystallization of meloxicam represents a promising approach to diversify the novel crystal forms, which can then be used to improve the relevant aqueous solubility and accelerate the onset of action for mild or medium level pain relief. In this contribution, we use the supramolecular synthon approach to effectively prioritize all available cofomers and systematically prepare and characterize a variety of meloxicam cocrystals with carboxylic acids.

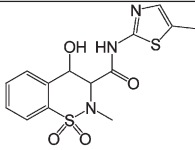
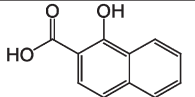
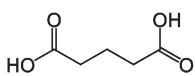
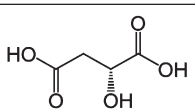
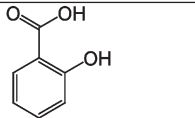
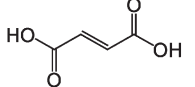
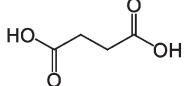
2. Materials and Methods

2.1. Materials. Meloxicam was purchased from Jai Radhe Sales, India, with a purity of 99.64% and was used without further purification. All other chemicals were supplied by Sigma-Aldrich and used without further purification.

2.2. Synthesis of Cocrystals 1–19. Meloxicam was reacted with 18 selected cofomers: 1-hydroxy-2-naphthoic acid, glutaric acid, L-malic acid, salicylic acid, fumaric acid, succinic acid, maleic acid, malonic acid, gentisic acid, 4-hydroxybenzoic acid, adipic acid, (+)-camphoric acid, glycolic acid, benzoic acid, DL-malic acid, hydrocinnamic acid, ascorbic acid, and L-tartaric acid. All cofomers (Tables 1 and 2) except ascorbic acid and L-tartaric acid produced at least one meloxicam cocrystal form. The cocrystallization attempts resulted in 19 crystal forms, many of which were prepared via multiple synthetic techniques including solvent-drop grinding¹⁸ and slurring. Single crystals suitable for X-ray diffraction were successfully prepared for six of the 19 cocrystals (1–6).

Synthesis of Meloxicam·1-Hydroxy-2-naphthoic Acid (1:1) Cocrystal (1). (a) Solvent-drop grinding: 0.176 g (0.501 mmol) of meloxicam was ground with 0.0957 g (0.508 mmol) of 1-hydroxy-2-naphthoic acid and 40 μ L of tetrahydrofuran (THF) for 30 min in a ball-mill. Cocrystal 1 was generated in ca. 100% yield. (b) Slurry: 0.700 g (1.99 mmol) of meloxicam and 0.391 g (2.07 mmol) of 1-hydroxy-2-naphthoic acid were slurried at ca. 250 rpm in 3 mL of THF overnight sealed under ambient conditions. The resulting solid was filtered and washed with THF. Cocrystal 1 was obtained in ca. 90% yield. (c) Solution Crystallization: 0.0176 g (0.0501 mmol) of

Table 1. Molecular Structure, pK_a ,^{49,50} ΔpK_a , and Melting Point Values for Meloxicam and Coformers That Form Cocrystals 1–6

Name	Molecular structure	pK_a (pK_{a1})	ΔpK_a	Ratio Meloxicam : Coformer	Melting point of coformer (°C)	Melting point of cocrystal (°C)
Meloxicam		4.18	N/A	N/A	254	N/A
1-Hydroxy-2-naphthoic Acid (coformer in 1)		3.02	1.16	1:1	195	225
Glutaric Acid (coformer in 2)		4.34	-0.16	1:1	95	149
L-Malic Acid (coformer in 3)		3.46	0.72	1:1:1 (meloxicam cation: meloxicam: L-malate)	101	200
Salicylic Acid Form III (coformer in 4)		2.97	1.21	1:1	159	210
Fumaric Acid (coformer in 5)		3.1	1.08	2:1	287	240
Succinic Acid (coformer in 6)		4.19	-0.01	2:1	185	226

meloxicam and 0.0095 g (0.0505 mmol) of 1-hydroxy-2-naphthoic acid were dissolved in 10 mL of ethyl acetate and left to slowly evaporate. Cocrystal **1** was obtained in ca. 93% yield.

Synthesis of Meloxicam·Glutaric Acid (1:1) Cocrystal (2). (a) Solvent-drop grinding: 0.179 g (0.511 mmol) of meloxicam was ball-milled with 0.0699 g (0.529 mmol) of glutaric acid and 40 μ L of chloroform for 30 min, producing **2** in ca. 100% yield. (b) Slurry: 0.892 g (2.54 mmol) of meloxicam and 0.351 g (2.66 mmol) of glutaric acid were slurried at ca. 250 rpm in 3 mL of ethyl acetate overnight sealed under ambient conditions. The resulting solid was filtered and washed with ethyl acetate. Cocrystal **2** was made in ca. 96% yield. (c) Solution crystallization: 0.0194 g (0.0552 mmol) of meloxicam and 0.159 g (1.20 mmol) of glutaric acid were dissolved in 2 mL of ethyl acetate and left to slowly evaporate. Cocrystal **2** was isolated in ca. 89% yield.

Synthesis of Meloxicam·L-Malic Acid (1:1:1) Cocrystal of a Salt (3). (a) Solvent-drop grinding: 0.176 g (0.501 mmol) of meloxicam was ground together with 0.0361 g (0.269 mmol) of L-malic acid and 40 μ L of THF for 30 min in a mechanical ball-mill. Cocrystal **3** was generated in ca. 100% yield. (b) Slurry: 0.897 g (2.55 mmol) of meloxicam and 0.182 g (1.36 mmol) of L-malic acid were slurried at ca. 250 rpm in 3 mL of THF overnight sealed under ambient conditions. The resulting solid was filtered and washed with THF and afforded a ca. 92% yield of **3**. (c) Solution crystallization: 0.0214 g (0.0609 mmol) of meloxicam and 0.0416 g (0.301 mmol) of L-malic acid were dissolved in 2 mL of a 1:1 mix of 1,4-dioxane and ethyl acetate and left to slowly evaporate. The resulting single crystals of **3** were isolated in ca. 82% yield.

Synthesis of Meloxicam·Salicylic Acid (1:1) Cocrystal Form III (4). (a) Solvent-drop grinding: 0.174 g (0.495 mmol) of meloxicam was ball-milled with 0.0724 g (0.524 mmol) of salicylic acid and 40 μ L of ethyl acetate for 30 min. Cocrystal **4** was synthesized in ca. 100% yield. (b) Slurry: 0.876 g (2.49 mmol) of meloxicam and 0.350 g (2.53 mmol) of salicylic acid were slurried at ca. 250 rpm in 2 mL of

THF overnight sealed under ambient conditions. The resulting solid was filtered and washed with THF. Cocrystal **4** was isolated in ca. 84% yield. (c) Solution crystallization: 0.0226 g (0.0643 mmol) of meloxicam and 0.0787 g (0.570 mmol) of salicylic acid were dissolved in 8 mL of a 6:2 mixture of ethyl acetate and 1,4-dioxane and left to slowly evaporate. Single crystals of **4** (ca. 33% yield) grew concomitantly with meloxicam form I and salicylic acid.

Synthesis of Meloxicam·Fumaric Acid (2:1) Cocrystal (5). (a) Solvent-drop grinding: 0.088 g (0.250 mmol) of meloxicam was ball-milled with 0.015 g (0.129 mmol) of fumaric acid and 50 μ L of THF for 30 min, generating **5** in ca. 100% yield. (b) Slurry: 0.880 g (2.50 mmol) of meloxicam and 0.150 g (1.29 mmol) of fumaric acid were slurried at ca. 250 rpm in 3 mL of THF overnight sealed under ambient conditions. The resulting solid was filtered and washed with THF. Cocrystal **5** was isolated in ca. 81% yield. (c) Solution crystallization: 0.100 g (0.284 mmol) of meloxicam and 0.330 g (0.284 mmol) of fumaric acid were dissolved in 9 mL of a THF and left to slowly evaporate resulting in single crystals of **5** (ca. 31% yield).

Synthesis of Meloxicam·Succinic Acid (2:1) Cocrystal (6). (a) Solvent-drop grinding: 0.088 g (0.250 mmol) of meloxicam was ball-milled with 0.015 g (0.127 mmol) of succinic acid and 50 μ L of THF for 30 min, generating **6** in ca. 100% yield. (b) Slurry: 0.880 g (2.50 mmol) of meloxicam and 0.150 g (1.27 mmol) of succinic acid were slurried at ca. 250 rpm in 3 mL of THF overnight sealed under ambient conditions. The resulting solid was filtered and washed with THF. Cocrystal **6** was isolated in ca. 78% yield. (c) Solution crystallization: 0.100 g (0.284 mmol) of meloxicam and 0.017 g (0.142 mmol) of succinic acid was dissolved in 10 mL of 1:1 THF and left to slowly evaporate. Single crystals of **6** (ca. 55% yield) grew concomitantly with meloxicam form I and succinic acid.

Synthesis of Meloxicam·Salicylic Acid (1:1) Cocrystal Form I (7). (a) Solvent-drop grinding: 0.177 g (0.504 mmol) of meloxicam was ball-milled with 0.0675 g (0.489 mmol) of salicylic acid and 40 μ L of

Table 2. Molecular Structures, pK_a ,^{49,51} ΔpK_a , and Melting Point Values for Coformers That Form Cocrystals 7–19

Name	Molecular structure	pK_a (pK_{a1})	ΔpK_a	Ratio Meloxicam: Coformer	Melting point of coformer (°C)	Melting point of cocrystal (°C)
Salicylic Acid Form I (7)		2.97	1.21	1:1	159	205
Salicylic Acid Form II (8)		2.97	1.21	1:1	159	206
Maleic Acid (9)		1.93	2.25	1:1	137	192
Malonic Acid (10)		2.83	1.35	1:1	134	164
Gentisic Acid (11)		2.98	1.20	1:1	203	237
4-Hydroxybenzoic Acid (12)		4.58	-0.40	1:1	214	209
Adipic Acid (13)		4.42	-0.24	2:1	152	209
(+)-Camphoric Acid (14)		4.70	-0.52	1:1	183	194
(+)-Camphoric Acid (15)		4.70	-0.52	3:2	183	212
Glycolic Acid (16)		3.83	0.35	1:1	75	163
Benzoic Acid (17)		4.20	-0.02	1:1	122	189
DL-Malic Acid (18)		3.40	0.78	2:1	131	215
Hydrocinnamic Acid (19)		4.66	-0.48	1:1	48	137

THF for 30 min. Cocrystal 7 was isolated in ca. 100% yield. (b) Slurry: 0.871 g (2.47 mmol) of meloxicam and 0.352 g (2.55 mmol) of salicylic acid were slurried at ca. 250 rpm in 2 mL of methanol overnight sealed under ambient conditions. The resulting solid was filtered and washed with methanol. Cocrystal 7 was obtained in ca. 91% yield.

Synthesis of Meloxicam·Salicylic Acid (1:1) Cocrystal Form II (8). (a) Solvent-drop grinding: 0.175 g (0.498 mmol) of meloxicam was ball-milled with 0.0705 g (0.510 mmol) of salicylic acid and 40 μ L of chloroform for 30 min, generating **8** in ca. 100% yield. (b) Slurry: 0.869 g (2.47 mmol) of meloxicam and 0.356 g (2.58 mmol) of salicylic acid were slurried at ca. 250 rpm in 2 mL of chloroform overnight sealed under ambient conditions. The resulting solid was filtered and washed with chloroform. Cocrystal **8** was isolated in ca. 89% yield.

Synthesis of Meloxicam·Maleic Acid (1:1) Cocrystal (9). (a) Solvent-drop grinding: 0.175 g (0.498 mmol) meloxicam was ball-milled with 0.058 g (0.498 mmol) of maleic acid and 40 μ L of THF for 30 min, generating **9** in ca. 100% yield. (b) Slurry: 0.750 g (2.13 mmol) of meloxicam and 0.248 g (2.13 mmol) of maleic acid were slurried at ca. 250 rpm in 2 mL of THF overnight sealed under ambient conditions. The resulting solid was filtered and washed with the same solvent employed for the slurry. Cocrystal **9** was isolated in ca. 92% yield. Cocrystal **9** can also be synthesized via ethyl acetate slurry.

Synthesis of Meloxicam·Malonic Acid (1:1) Cocrystal (10). (a) Solvent-drop grinding: 0.175 g (0.498 mmol) of meloxicam was ball-milled with 0.052 g (0.498 mmol) of malonic acid and 40 μ L of THF for 30 min, generating **10** in ca. 100% yield. (b) Slurry: 0.900 g

Table 3. Crystal Structure Parameters for Cocrystals 1–6

	1	2	3	4	5	6
chemical formula	$C_{14}H_{13}N_3O_4S_2 \cdot C_{11}H_8O_3$	$C_{14}H_{13}N_3O_4S_2 \cdot C_5H_8O_4$	$C_{14}H_{13}N_3O_4S_2 \cdot C_{14}H_{13}N_3O_4S_2 \cdot S_2 \cdot C_4H_5O_5$	$C_{14}H_{13}N_3O_4S_2 \cdot C_7H_6O_3$	$C_{14}H_{13}N_3O_4S_2 \cdot C_{14}H_{13}N_3O_4S_2 \cdot S_2 \cdot C_4H_4O_4$	$(C_{14}H_{13}N_3O_4S_2)_2 \cdot C_4H_6O_4$
formula weight	539.57	483.51	836.88	489.51	818.86	820.88
cryst syst	triclinic	triclinic	triclinic	monoclinic	triclinic	triclinic
space group	$P\bar{1}$	$P\bar{1}$	$P1$	$P2_1/c$	$P\bar{1}$	$P\bar{1}$
<i>a</i> (Å)	6.938(3)	7.181(2)	7.278(2)	11.0844(5)	7.145(5)	7.2315(4)
<i>b</i> (Å)	11.997(5)	8.439(3)	8.550(2)	11.8433(5)	8.475(5)	8.4994(5)
<i>c</i> (Å)	15.107(6)	18.364(6)	15.150(4)	16.4532(7)	15.088(9)	14.9383(8)
α (deg)	112.838(5)	80.737(4)	84.115(3)	90	82.250(9)	82.741(4)
β (deg)	92.889(6)	85.464(4)	81.617(4)	97.386(3)	81.368(9)	80.061(3)
γ (deg)	95.816(6)	70.865(4)	70.489(3)	90	70.519(9)	70.313(4)
vol (Å ³)	1147.4(8)	1037.2(6)	877.6(4)	2141.99(16)	848.1(7)	849.21(8)
<i>D</i> _{calcd} (g cm ^{−3})	1.562	1.548	1.583	1.518	1.603	1.605
<i>Z</i>	2	2	1	4	1	1
reflns collected	5872	5390	4334	11932	4399	5052
independent reflns	4079	3688	3037	3532	3031	2719
obsd reflns	3249	3298	1620	2659	2298	1871
<i>T</i> (K)	100	100	293	293	100	100
<i>R</i> ₁	0.0511	0.0338	0.0663	0.0433	0.0451	0.0463
<i>wR</i> ₂	0.1200	0.0894	0.1138	0.1103	0.1067	0.0845
GOF	1.058	1.049	0.986	1.010	0.995	0.995

(2.56 mmol) of meloxicam and 0.266 g (2.56 mmol) of malonic acid were slurried at ca. 250 rpm in 2 mL of THF overnight sealed under ambient conditions. The resulting solid was filtered and washed with THF. Cocrystal **10** was isolated in ca. 88% yield.

Synthesis of Meloxicam·Gentisic Acid (1:1) Cocrystal (11). (a) Solvent-drop grinding: 0.175 g (0.498 mmol) of meloxicam was ball-milled with 0.077 g (0.498 mmol) of gentisic acid and 40 μ L of chloroform or THF for 30 min, generating **11** in ca. 100% yield. (b) Slurry: 0.850 g (2.41 mmol) of meloxicam and 0.373 g (2.41 mmol) of gentisic acid were slurried at ca. 250 rpm in 2 mL of chloroform overnight sealed under ambient conditions. The resulting solid was filtered and washed with the same solvent employed for the slurry. Cocrystal **11** was isolated in ca. 85% yield. Cocrystal **11** can also be synthesized via slurry in ethyl acetate.

Synthesis of Meloxicam·4-Hydroxybenzoic Acid (1:1) Cocrystal (12). Solvent-drop grinding: 0.175 g (0.498 mmol) of meloxicam was ball-milled with 0.069 g (0.498 mmol) of 4-hydroxybenzoic acid and 40 μ L of THF for 30 min, generating **12** in ca. 100% yield.

Synthesis of Meloxicam·Adipic Acid (2:1) Cocrystal (13). (a) Solvent-drop grinding: 0.088 g (0.250 mmol) of meloxicam was ball-milled with 0.018 g (0.123 mmol) of adipic acid and 50 μ L of THF for 30 min, generating **13** in ca. 100% yield. (b) Slurry: 0.880 g (2.50 mmol) of meloxicam and 0.180 g (1.23 mmol) of adipic acid were slurried at ca. 250 rpm in 3 mL of THF overnight sealed under ambient conditions. The resulting solid was filtered and washed with THF. Cocrystal **13** was isolated in ca. 80% yield.

Synthesis of Meloxicam·(+)-Camphoric Acid (1:1) Cocrystal (14). Solvent-drop grinding: 0.175 g (0.498 mmol) of meloxicam was ball-milled with 0.100 g (0.498 mmol) of (+)-camphoric acid and 40 μ L of THF for 30 min, generating **14** in ca. 100% yield.

Synthesis of Meloxicam·(+)-Camphoric Acid (3:2) Cocrystal (15). Slurry: 0.700 g (1.99 mmol) of meloxicam and 0.266 g (1.33 mmol) of (+)-camphoric acid were slurried at ca. 250 rpm in 4 mL of chloroform overnight sealed under ambient conditions. The resulting solid was filtered and washed with chloroform. Cocrystal **15** was isolated in ca. 91% yield.

Synthesis of Meloxicam·Glycolic Acid (1:1) Cocrystal (16). (a) Solvent-drop grinding: 0.175 g (0.498 mmol) of meloxicam was ball-milled with 0.038 g (0.498 mmol) of glycolic acid and 40 μ L of chloroform for 30 min, generating **16** in ca. 100% yield. (b) Slurry: 0.950 g (2.70 mmol) of meloxicam and 0.206 g (2.70 mmol) of glycolic acid were slurried at ca. 250 rpm in 2 mL of ethyl acetate overnight sealed under ambient conditions. The resulting solid was filtered and washed with ethyl acetate. Cocrystal **16** was isolated in ca. 92% yield.

Synthesis of Meloxicam·Benzoic Acid (1:1) Cocrystal (17). (a) Solvent-drop grinding: 0.176 g (0.501 mmol) of meloxicam was ball-milled with 0.061 g (0.500 mmol) of benzoic acid and 50 μ L of THF for 30 min, generating **17** in ca. 100% yield. (b) Slurry: 0.176 g (0.501 mmol)

of meloxicam and 0.061 g (0.500 mmol) of benzoic acid were slurried at ca. 250 rpm in 3 mL of ethyl acetate overnight sealed under ambient conditions. The resulting solid was filtered and washed with ethyl acetate. Cocrystal **17** was isolated in ca. 81% yield.

Synthesis of Meloxicam·DL-Malic Acid (2:1) Cocrystal (18). (a) Solvent-drop grinding: 0.088 g (0.250 mmol) of meloxicam was ball-milled with 0.017 g (0.127 mmol) of DL-malic acid and 50 μ L of THF for 30 min, generating **18** in ca. 100% yield. (b) Slurry: 0.880 g (2.50 mmol) of meloxicam and 0.170 g (1.27 mmol) of DL-malic acid were slurried at ca. 250 rpm in 3 mL of THF overnight sealed under ambient conditions. The resulting solid was filtered and washed with THF. Cocrystal **18** was isolated in ca. 79% yield.

Synthesis of Meloxicam·Hydrocinnamic Acid (1:1) Cocrystal (19). (a) Solvent-drop grinding: 0.176 g (0.501 mmol) of meloxicam was ball-milled with 0.075 g (0.499 mmol) of hydrocinnamic acid and 50 μ L of THF for 30 min, generating **19** in ca. 100% yield. (b) Slurry: 0.702 g (2.00 mmol) of meloxicam and 0.300 g (1.99 mmol) of hydrocinnamic acid were slurried at ca. 250 rpm in 3 mL of ethyl acetate overnight sealed under ambient conditions. The resulting solid was filtered and washed with ethyl acetate. Cocrystal **19** was isolated in ca. 78% yield.

2.3. Crystal Form Characterization. Single-Crystal X-ray Diffraction. Quality single crystals for X-ray diffraction were obtained for six compounds. Attempts to crystallize **7–19** did not afford crystals suitable for single-crystal X-ray crystallographic analysis. Single crystal analysis for **1–3** was performed on a Bruker-AXS SMART APEX CCD diffractometer with monochromatized Mo K α radiation ($\lambda = 0.71073$ Å) connected to a KRYO-FLEX low-temperature device, while data for **4–6** were collected using Cu K α radiation ($\lambda = 1.54178$ Å). Data for **1, 2, 5, and 6** were collected at 100 K. Data for **3** and **4** were collected at 293 K (Table 3). Lattice parameters were determined from least-squares analysis, and reflection data were integrated using SAINT.³⁸ Structures were solved by direct methods and refined by full matrix least-squares based on F^2 using the SHELXTL package.³⁹ All non-hydrogen atoms were refined with anisotropic displacement parameters. All hydrogen atoms bonded to carbon, nitrogen, and oxygen atoms were placed geometrically and refined with an isotropic displacement parameter fixed at 1.2U_{eq} of the atoms to which they were attached. Hydrogen atoms bonded to methyl groups were placed geometrically and refined with an isotropic displacement parameter fixed at 1.5U_{eq} of the carbon atoms.

Powder X-ray Diffraction (PXRD). Cocrystals **1–19** were characterized using a D-8 Bruker X-ray powder diffractometer using Cu K α radiation ($\lambda = 1.54178$ Å), 40 kV, 40 mA. Data were collected over an angular range of 3°–40° 2 θ value in continuous scan mode using a step size of 0.05° 2 θ value and a scan rate of 5°/min.

Calculated PXRD. Calculated PXRD diffractograms were generated from the single-crystal structures of **1–6** using Mercury

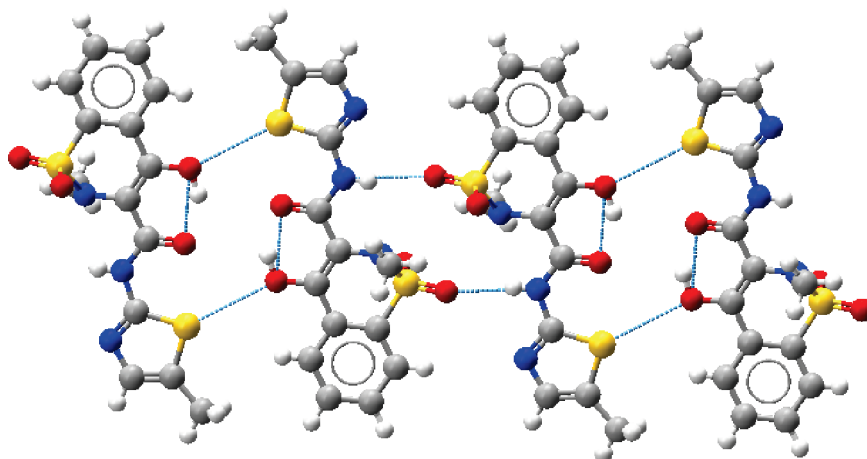


Figure 1. Meloxicam supramolecular chains sustained by sulfonyl–amide dimers and sulfathiazole–alcohol supramolecular synthons.

2.2 (Cambridge Crystallographic Data Centre, UK) for the following complexes and compared with the pattern obtained for the corresponding bulk sample.

Differential Scanning Calorimetry (DSC). Differential scanning calorimetry was performed on a Perkin-Elmer Diamond DSC with a typical scan range of 25–280 °C, scan rate of 10 °C/min, and nitrogen purge of ca. 30 psi.

Fourier Transform Infrared Spectroscopy (FT-IR). FT-IR analysis was performed on a Perkin-Elmer Spectrum 100 FT-IR spectrometer equipped with a solid-state ATR accessory.

3. Results and Discussion

3.1. The Supramolecular Synthon Approach. As previously mentioned, a key step in generating pharmaceutical cocrystals is to analyze the target API from a crystal engineering perspective, to evaluate how the target molecule would form supramolecular synthons. This methodology partitions the target molecule by its functional groups and statistically⁴⁰ examines the percentage of occurrence of supramolecular homo- and heterosynthons for these functional groups. The targeted supramolecular synthons are typically sustained via hydrogen bonds because they are strong and directional in nature. This method is particularly beneficial because most APIs tend to be rich in functional groups that are capable of forming strong hydrogen bonds.

Polymorphic form I⁴¹ of meloxicam (refcode SEDZOQ) indicates that meloxicam molecules form supramolecular chains that are sustained by sulfonyl–amide and sulfathiazole–alcohol supramolecular heterosynthons, as shown in Figure 1. The chains are held together by various weak interactions, stacking along the *a*-axis in a slipped fashion. Thus for meloxicam cocrystallization, one or all of these supramolecular synthon motifs must be interrupted.³⁷

3.1.1. CSD Analysis. A CSD analysis⁴² was conducted to examine the occurrence of supramolecular synthon formation of the amino-azole functionality (five-membered ring containing a nitrogen and primary amine) with carboxylic acid, primary amide, and alcohol moieties. It was noted that many of the searches for the amino-azole moiety coupled with an additional functional group consisted of a relatively small number of entries. Any conclusions from the data might therefore be statistically insignificant. Therefore further CSD analysis was conducted employing a simple azole (five-membered ring containing one nitrogen atom and at least one additional heteroatom). The reliability of supramolecular heterosynthon versus homosynthon formation

between an azole and a carboxylic acid, primary amide, and alcohol were examined using the CSD. Due to the inability of the azole to form a supramolecular synthon with itself, only the homosynthon formation of the carboxylic acid, primary amide, and alcohol moieties in the presence of an azole was examined. Meanwhile, it was noted that when the pK_a difference (ΔpK_a , $\Delta pK_a = pK_a(\text{base}) - pK_a(\text{acid})$) between meloxicam and a carboxylic acid coformer is significant, the coformer could protonate meloxicam and form a carboxylate salt. With this in mind, carboxylate–azole interactions were also searched in the CSD. The analysis showed that the azole–carboxylic acid and azole–alcohol supramolecular heterosynthons are persistent (see Supporting Information).

3.1.2. Selection of Meloxicam Coformers. Based on the statistical success rate of supramolecular heterosynthon formation between azoles and carboxylic acids, a meloxicam cocrystal screen with acidic coformers that are pharmaceutically acceptable or toxicologically qualified was conducted. The focus of the study was rather narrow in scope and did not include coformers that only possessed alcohol moieties despite the potential for interaction based upon the CSD statistics. Meloxicam was thereby reacted with 1-hydroxy-2-naphthoic acid, glutaric acid, L-malic acid, salicylic acid, fumaric acid, succinic acid, maleic acid, malonic acid, gentisic acid, 4-hydroxybenzoic acid, adipic acid, (+)-camphoric acid, glycolic acid, benzoic acid, DL-malic acid, hydrocinamic acid, ascorbic acid, and L-tartaric acid. All coformers except ascorbic acid and L-tartaric acid produced at least one cocrystal. The cocrystallization attempts resulted in 19 crystal forms; namely, meloxicam·1-hydroxy-2-naphthoic acid cocrystal, meloxicam·glutaric acid cocrystal, meloxicam·L-malic acid cocrystal of a salt, meloxicam·salicylic acid cocrystal forms I, II, and III, meloxicam·fumaric acid cocrystal, meloxicam·succinic acid cocrystal, meloxicam·maleic acid cocrystal, meloxicam·malonic acid cocrystal, meloxicam·gentisic acid cocrystal, meloxicam·4-hydroxybenzoic acid cocrystal, meloxicam·adipic acid cocrystal, meloxicam·(+)-camphoric acid cocrystal (1:1), meloxicam·(+)-camphoric acid cocrystal (3:2), meloxicam·glycolic acid cocrystal, meloxicam·benzoic acid cocrystal, meloxicam·DL-malic acid cocrystal, and meloxicam·hydrocinamic acid cocrystal.

3.2. Crystal Structure Descriptions. **3.2.1. Meloxicam·1-Hydroxy-2-naphthoic Acid (1:1) Cocrystal, 1.** Meloxicam·1-hydroxy-2-naphthoic acid cocrystal (1) crystallizes in the

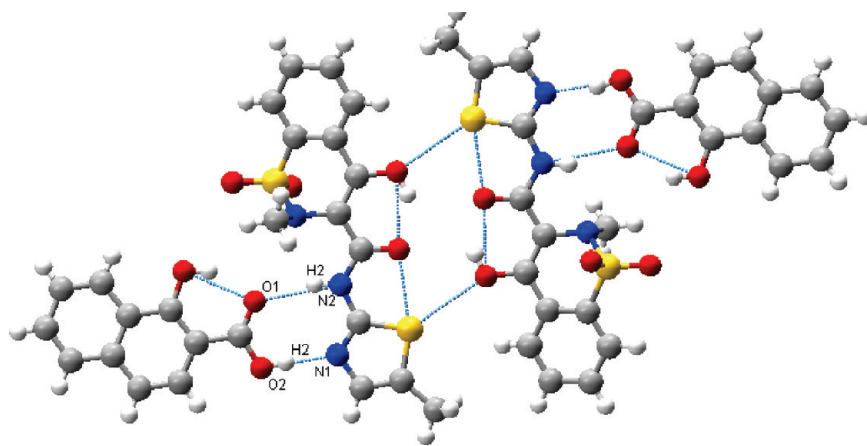


Figure 2. A supramolecular unit formed by meloxicam and 1-hydroxy-2-naphthoic acid in **1**.

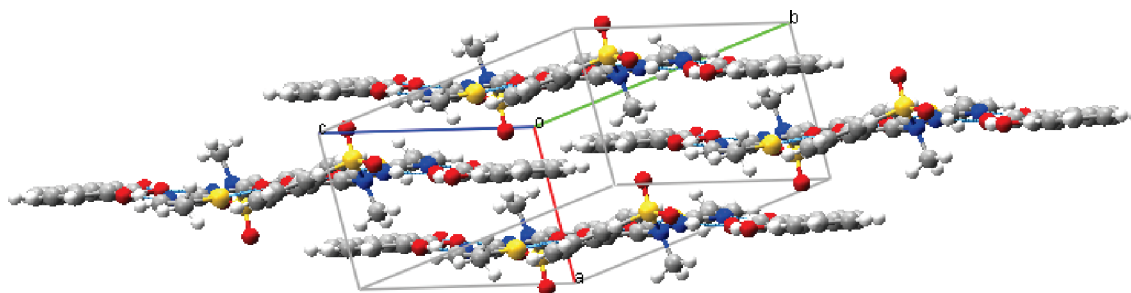


Figure 3. Packing of four supramolecular layers in **1**.

space group $P\bar{1}$. The asymmetric unit contains one meloxicam and one 1-hydroxy-2-naphthoic acid molecule. The primary supramolecular unit comprises two meloxicam molecules and two 1-hydroxy-2-naphthoic acid molecules with the inversion center located in the center of the meloxicam dimer (Figure 2). The meloxicam dimer is a common motif found in the structure of various meloxicam cocrystals and is sustained by two planar meloxicam molecules interacting via electrostatic interactions between the alcohol, ketone, and sulfathiazole moieties. It is observed that meloxicam sustains intramolecular alcohol–ketone interactions and binds to the neighboring meloxicam via an $S \cdots OH$ interaction at a distance of 3.111 Å to form the meloxicam dimer. The exterior of the meloxicam dimer hydrogen bonds to two 1-hydroxy-2-naphthoic acid molecules via two-point recognition carboxylic acid–thiazole/NH interactions [for $O2-H2 \cdots N1$, $O \cdots N$ 2.563(3) Å, $H \cdots N$ 1.728 Å, $O-H \cdots N$ 172.19°; for $N2-H2N \cdots O1$, $N \cdots O$ 2.902(3) Å, $H \cdots O$ 2.026 Å, $N-H \cdots O$ 166.48°]. This two-point supramolecular heterosynthon motif is quite robust since it is found in all crystallographically characterized cocrystal forms reported herein. The hydroxyl group of 1-hydroxy-2-naphthoic acid adjacent to the carboxylic acid moiety is involved in intramolecular hydrogen bonding, which is expected based upon Etter's rules.⁴³ The overall packing, illustrated in Figure 3, is sustained by the primary supramolecular units of meloxicam and 1-hydroxy-2-naphthoic acid that stack upon each other along the *a*-axis in a slipped fashion with an interplanar spacing of 3.630 Å.

3.2.2. Meloxicam·Glutaric Acid (1:1) Cocrystal, 2. The asymmetric unit of the meloxicam·glutaric acid cocrystal (**2**) comprises one meloxicam and one glutaric acid molecule (Figure 4). Cocrystal **2** crystallizes in the space group $P\bar{1}$. The meloxicam centrosymmetric dimer, which is again present in

2, is sustained by an $S \cdots OH$ interaction between two planar meloxicam molecules with a distance of 3.213 Å. In addition, an intramolecular $OH \cdots O$ hydrogen bond is also observed on meloxicam. Interestingly, glutaric acid utilizes one of its carboxylic acid moieties to form a centrosymmetric carboxylic acid dimer [$O4-H4 \cdots O3$: $O \cdots O$ 2.641(2) Å, $H \cdots O$ 1.801 Å, $O-H \cdots O$ 177.76°] with a neighboring glutaric acid. The other carboxylic acid moiety of glutaric acid hydrogen bonds to the adjacent meloxicam molecule, resulting in the unexpected 1:1 stoichiometry. The carboxylic acid–azole supramolecular heterosynthon dimer is sustained by hydrogen bond interactions that afford the common two-point recognition motif. The $OH \cdots N$ and $NH \cdots O$ interactions are shown in Figure 4 [for $O2-H2O \cdots N1$, $O \cdots N$ 2.6675(19) Å, $H \cdots N$ 1.831 Å, $O-H \cdots N$ 173.96°; for $N2-H2N \cdots O1$, $N \cdots O$ 2.838(2) Å, $H \cdots O$ 1.979 Å, $N-H \cdots O$ 164.95°]. The supramolecular homosynthon and heterosynthon dimers ultimately result in the formation of a zigzag supramolecular chain that cuts through the *ac*-plane. The chains, which stack along the *a*-axis, are separated by a distance of 3.465 Å. Figure 5 highlights the close packing of multiple chains with meloxicam dimers and glutaric acid dimers disposed in a columnar arrangement. The $C1-C2-C3-C4$ torsion angle of glutaric acid in **2** is atypical. It is noted that the $C1-C2-C3-C4$ torsion angle in both polymorphs of pure glutaric acid is ca. 170°, whereas in **2** this torsion angle is 52.97°. A CSD search for additional glutaric acid cocrystals afforded multiple hits. Among those, glutaric acid with smaller torsion angles occurs in only two other cocrystals, that is, caffeine·glutaric acid cocrystal (refcode EXUQUJ) and theophylline·glutaric acid cocrystal (refcode XEJXIU), which exhibit torsion angles of 79.34° and 65.18°, respectively.

3.2.3. Meloxicam·L-Malic Acid (1:1:1) Cocrystal of a Salt, 3. The asymmetric unit of the meloxicam·L-malic acid

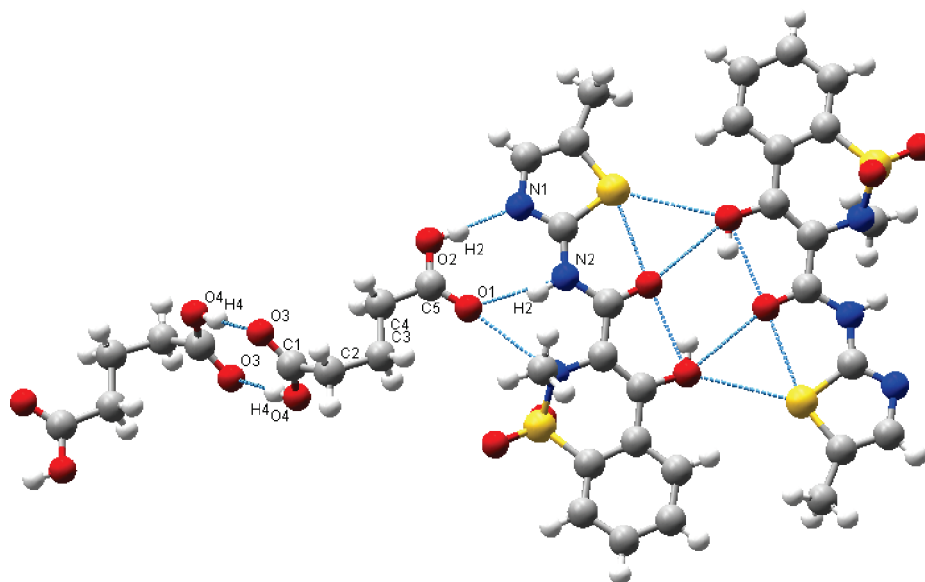


Figure 4. Supramolecular arrangements of meloxicam and glutaric acid dimers in **2**.

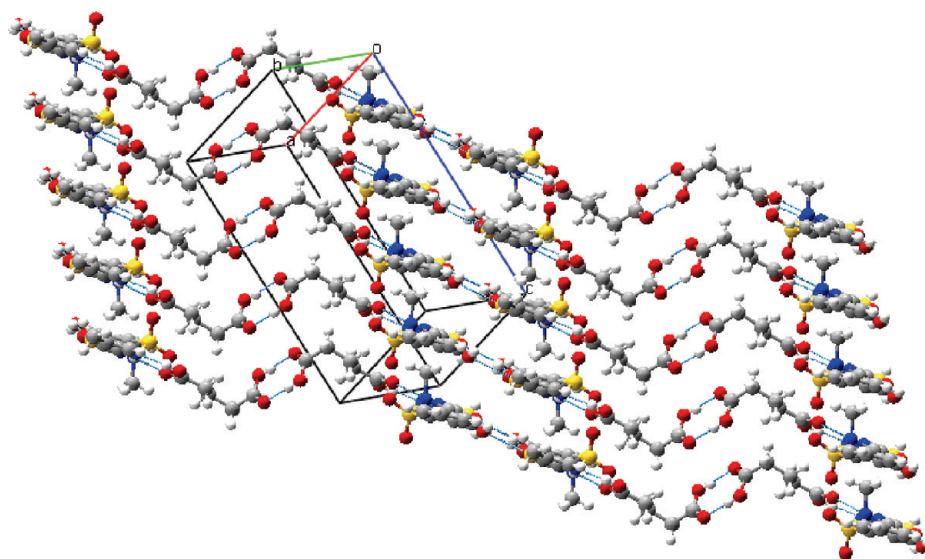


Figure 5. Packing of supramolecular chains in **2**.

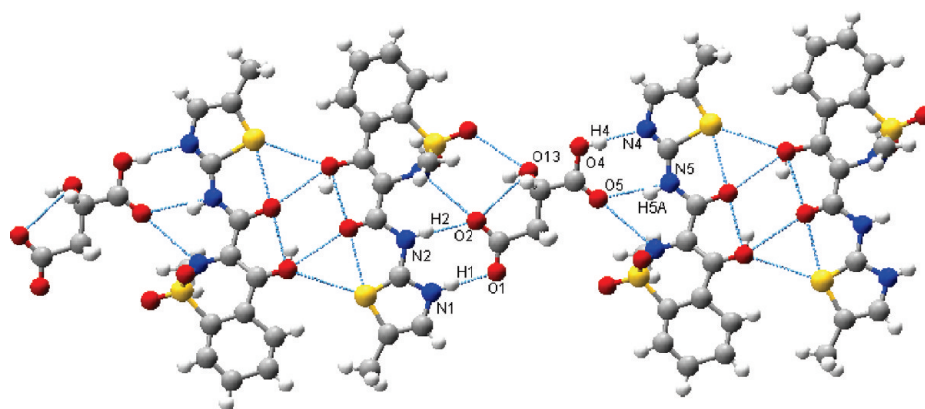


Figure 6. Supramolecular synthons in **3** showing a neutral and cationic meloxicam and an anionic L-malate.

cocrystal of a salt (**3**) contains one meloxicam cation, one neutral meloxicam, and one L-malate anion. Cocrystal **3** could therefore be considered a cocrystal of a salt and

crystallizes in the space group *P1*. Based upon the value of ΔpK_a (Table 1), it was unexpected that L-malic acid could protonate meloxicam. In **3**, the meloxicam dimer is

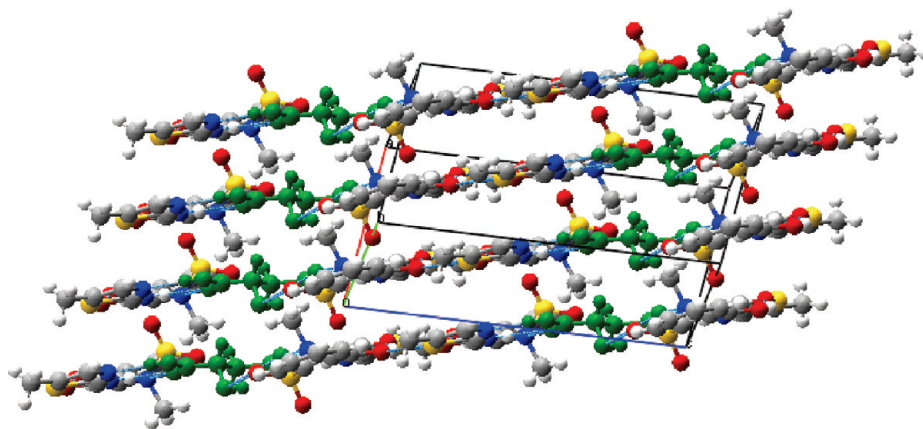


Figure 7. Stacked layers of **3**. L-Malate anions are highlighted in green.

comprised of one cation and one neutral meloxicam and is sustained by two $S \cdots OH$ interactions with $S \cdots O$ distances of 3.231 and 3.294 Å (Figure 6). Cocrystal **3** is also sustained by the L-malate anion acting as a bridge to connect the meloxicam dimers, ultimately forming a supramolecular chain. The L-malate bridge protonates the sulfathiazole ring via $O^- \cdots HN^+$ interactions [for $O1 \cdots H1N-N1$, $O^- \cdots N$ 2.686(17) Å, $H \cdots O$ 1.831 Å, $O \cdots H-N$ 173.33°; for $O2 \cdots H2N-N2$, $O \cdots N$ 2.948(16) Å, $H \cdots O$ 2.111 Å, $O \cdots H-N$ 164.78°] and hydrogen bonds to the sulfathiazole of the neutral meloxicam via $OH \cdots N$ and $NH \cdots O$ interactions [for $O4-H4O \cdots N4$, $O \cdots N$ 2.732(17) Å, $H \cdots N$ 1.915 Å, $O-H \cdots N$ 173.45°; for $O5 \cdots H5A-N5$, $O \cdots N$ 2.831(17) Å, $H \cdots O$ 1.989 Å, $O-H \cdots N$ 166.48°]. The supramolecular chains exhibited by **3** are reminiscent of those seen in **2**. L-Malate and meloxicam adopt a three-dimensional (3D) arrangement that comprises chains stacking parallel along the *a*-axis with a separation distance of 3.562 Å (centroid to plane), as shown in Figure 7.

3.2.4. Meloxicam·Salicylic Acid (1:1) Cocrystal Form III, 4. The supramolecular unit of meloxicam·salicylic acid cocrystal form III (**4**) comprises one molecular meloxicam and one molecular salicylic acid, shown in Figure 8. Cocrystal **4** crystallizes in the space group $P2_1/c$. Salicylic acid and meloxicam are associated by a supramolecular heterosynthon between the carboxylic acid and the sulfathiazole/NH moieties. The interactions of carboxylic acid with sulfathiazole/NH moiety include the $OH \cdots N$ hydrogen bond [$O2-H2O \cdots N1$, $O \cdots N$ 2.619(3) Å, $H \cdots N$ 1.807 Å, $O-H \cdots N$ 170.36°] and the $NH \cdots O$ hydrogen bond [$N2-H2N \cdots O1$, $N \cdots O$ 2.968(3) Å, $H \cdots O$ 2.133 Å, $N-H \cdots O$ 163.78°]. This hydrogen bonding motif generates a discrete unit containing one meloxicam and one salicylic acid molecule. In addition, intramolecular hydrogen bonding is observed on salicylic acid between the OH moiety and the carboxylic acid. Supramolecular units comprising meloxicam and salicylic acid in **4** translate along the 2_1 screw axis at a dihedral angle of 88.27° (Figure 9). Interestingly, the meloxicam dimer does not exist in **4** because the meloxicam molecules are perpendicular to adjacent meloxicam molecules. Cocrystal **4** is the only cocrystal reported herein that does not exhibit the meloxicam dimer. Two other meloxicam·salicylic acid cocrystal polymorphs (form I and form II) were also isolated, but single crystals suitable for single-crystal XRD analysis were not obtained.

3.2.5. Meloxicam·Fumaric Acid (2:1) Cocrystal, 5. The asymmetric unit of the meloxicam·fumaric acid cocrystal (**5**), which crystallizes in the space group $P\bar{1}$, contains two

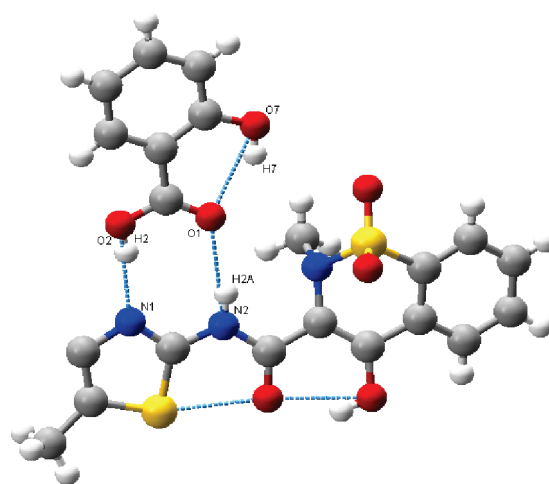


Figure 8. Two-point recognition supramolecular synthon in **4**.

meloxicam molecules and one fumaric acid molecule. In **5**, the meloxicam dimer persists and links to adjacent dimers via fumaric acid molecules, creating an infinite supramolecular chain (Figure 10). The supramolecular heterosynthon comprising carboxylic acid and sulfathiazole/NH moieties is observed between fumaric acid and meloxicam. Both $O-H \cdots N$ and $NH \cdots O$ hydrogen bonds are observed [$O22-H22O \cdots N3$, $O \cdots N$ 2.68(3) Å, $H \cdots N$ 1.821 Å, $O-H \cdots N$ 174.39°; $N2-H2N \cdots O21$, $N \cdots O$ 2.857(4) Å, $H \cdots O$ 1.976 Å, $N-H \cdots O$ 160.49°]. The supramolecular chain of meloxicam and fumaric acid exhibited in **5** is again similar to those observed in **2** and **3**. Clearly, the use of dicarboxylic acids with similar molecular structure orients meloxicam and cofomers similarly in the crystal lattice (Figure 11).

3.2.6. Meloxicam·Succinic Acid (2:1) Cocrystal, 6. Preparation of the meloxicam·succinic acid cocrystal (**6**) by solvent-drop grinding has been recently reported but without determination of its crystal structure.³⁶ The calculated PXRD of **6** based upon our single-crystal structure data matches that of the previously reported PXRD. Cocrystal **6** crystallizes in the space group $P\bar{1}$ with the asymmetric unit containing one meloxicam molecule and half a succinic acid molecule. The crystal structure of **6** reveals that the meloxicam dimers are associated with adjacent dimers by succinic acid molecules forming infinite supramolecular chains (Figure 12). Similar to previous meloxicam cocrystal structures, the primary intermolecular interactions of **6** are hydrogen bonds between meloxicam and succinic acid via the

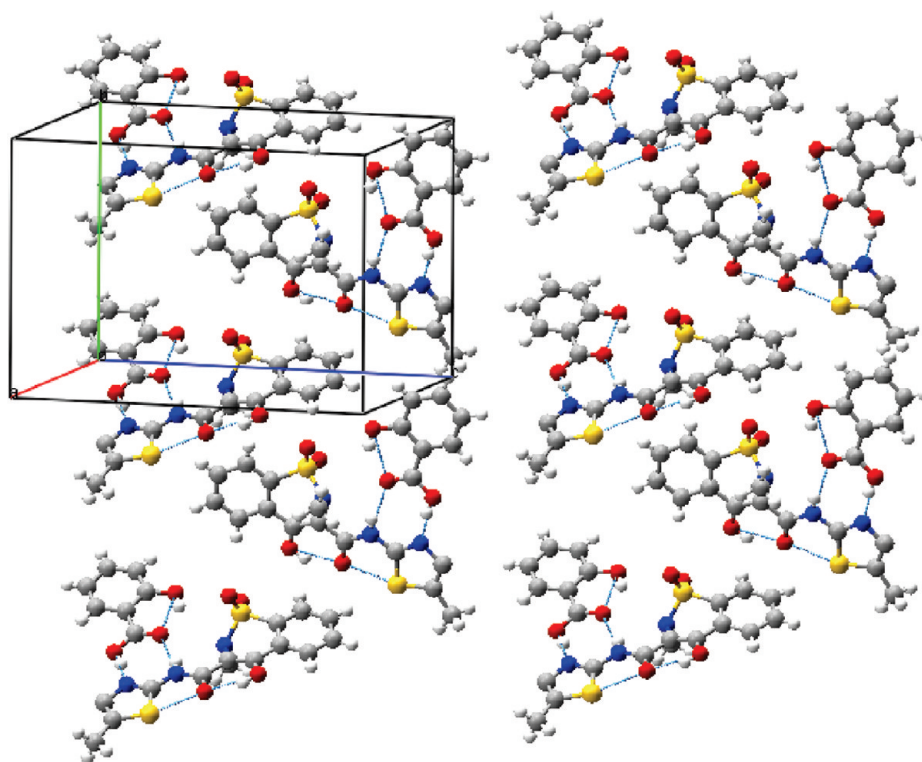


Figure 9. Supramolecular units comprising meloxicam and salicylic acid translating along the 2_1 screw axis.

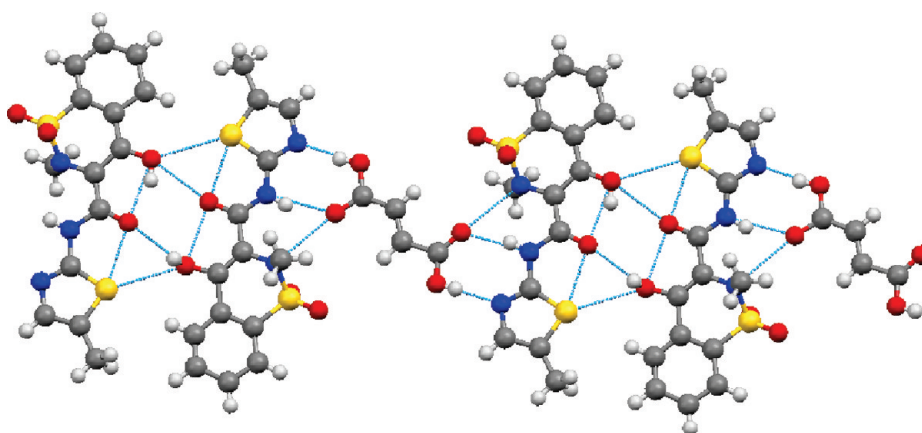


Figure 10. Supramolecular synthons observed in **5**.

carboxylic acid to sulfathiazole/NH supramolecular heterosynthon. The $\text{OH}\cdots\text{N}$ and $\text{NH}\cdots\text{O}=\text{C}$ hydrogen bonds are involved [$\text{O7}\cdots\text{H7}\cdots\text{N3}$, $\text{O}\cdots\text{N}$ 2.863(4) Å, $\text{H}\cdots\text{N}$ 1.847 Å, $\text{O}\cdots\text{H}\cdots\text{N}$ 173.63°; $\text{N2}\cdots\text{H2}\cdots\text{O6}$, $\text{N}\cdots\text{O}$ 2.849(4) Å, $\text{H}\cdots\text{O}$ 1.993 Å, $\text{N}\cdots\text{H}\cdots\text{O}$ 164.32°]. The supramolecular chains of meloxicam and succinic acid in **6** are reminiscent of the supramolecular chains found in **2**, **3**, and **5** (Figure 12). As shown in Figure 13, supramolecular chains of succinic acid and meloxicam stack with an interplanar spacing of 3.386 Å. As a result of an overall packing comparison between meloxicam cocrystal structures, it is observed that **3**, **5**, and **6** are isostructural.

3.2.7. Meloxicam Cocrystals 7–19. Cocrystals **7–19** were prepared from solution or solid-state grinding methods. However, the absence of structural data for **7–19** is the result of unsuccessful solution-based growth of single crystals. Nevertheless, polycrystalline powders of **7–19** were

characterized by PXRD, FT-IR, and thermal techniques. Even without the single-crystal XRD data, the stoichiometries of **7–19** were determined as exemplified by **9**.

The PXRD and FT-IR profiles of **9** were provided in the literature, but the stoichiometry of meloxicam and maleic acid in **9** was not disclosed. Based on the potential supramolecular interactions of meloxicam, the most likely stoichiometry of meloxicam and coformer in **9** is either 1:1 or 1:2.

In order to determine the stoichiometry of **9**, THF slurries of physical mixtures of meloxicam and maleic acid in molar ratios of 2:1, 1:1, and 1:2 were performed at room temperature overnight. From each slurry experiment, the solid crystalline powder was separated, washed with THF and dried for characterization. The absence of pure maleic acid, water, or THF was confirmed based on the DSC analysis upon all three solid powders from slurries. PXRD characterization indicated that the solids generated from the 1:1 and

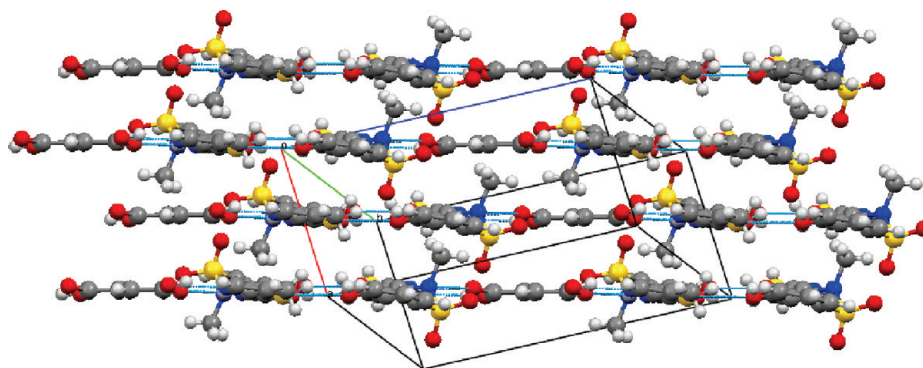


Figure 11. Supramolecular layers stacking in 5.

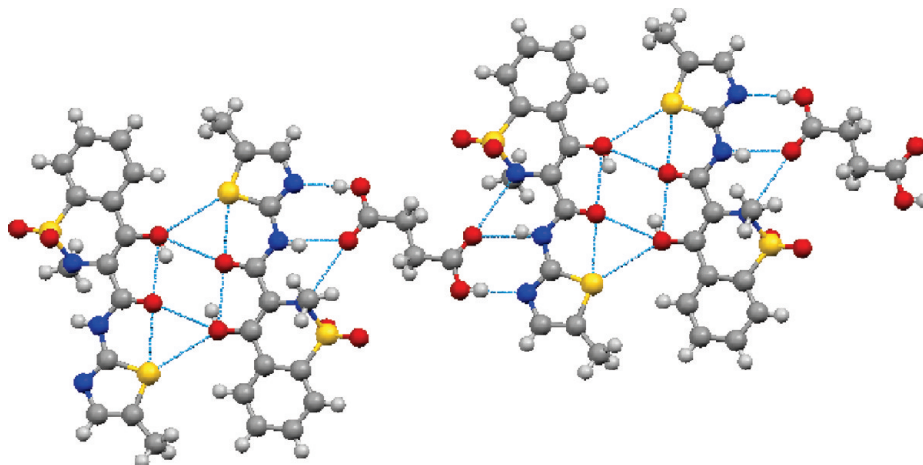


Figure 12. Supramolecular synthons observed in 6.

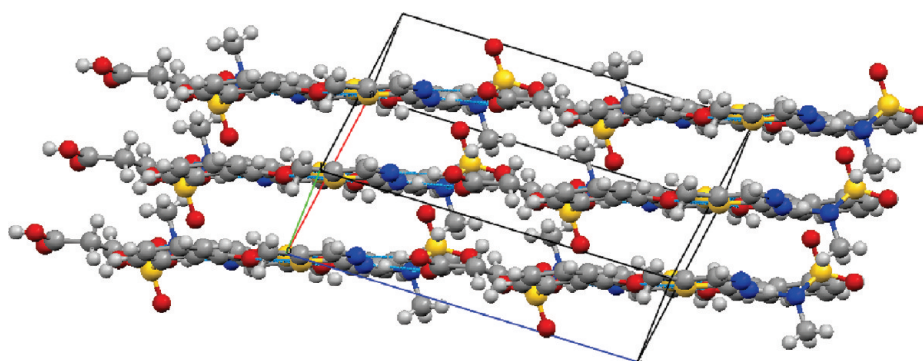


Figure 13. Supramolecular layers stacking in 6.

1:2 slurries were identical to the cocrystal form reported by Myz et al.³⁶ In contrast, the 2:1 slurry produced a physical mixture of meloxicam form I and the cocrystal. Further ¹H NMR analysis (400 MHz, *d*₆-DMSO) on solids from 1:1 and 1:2 slurries confirmed that the stoichiometry of meloxicam and maleic acid in 9 is 1:1 (see Supporting Information).

3.2.8. Meloxicam Crystal Forms: Cocrystals or Salts? Pharmaceutical cocrystals and salts are well-defined and are typically classified as distinct subsets of crystal forms. Whether novel meloxicam crystal forms generated by the 17 cofomers in this study are cocrystals or salts has also been investigated. For crystal forms with single-crystal XRD data (i.e., 1–6), the conclusion that 1–6 are cocrystals was drawn in a relatively simple and reliable manner. However, it was less straightforward to identify whether 7–19 are cocrystals or salts.

The pK_a values for meloxicam are 1.09 and 4.18.⁴⁴ The value of 1.09 is associated with the enolic OH group, while the value of 4.18 is linked to the nitrogen atom on the sulfathiazole ring. The enolic OH is much less accessible from a crystal engineering perspective because it is involved in intramolecular hydrogen bonding to the neighboring ketone or NH moieties. In contrast, the nitrogen atom on the sulfathiazole ring is the primary target for cocrystal or salt formation, because it could potentially sustain a supramolecular synthon with various hydrogen bond donors.

ΔpK_a is widely accepted as the key to predicting whether a salt or cocrystal form will form.^{45,46} It is generally considered that, if $\Delta pK_a < 0$, the resulting compound will be a cocrystal, whereas the result is typically a salt if $\Delta pK_a > 3$. For the region of ΔpK_a between $0 < \Delta pK_a < 3$, our ability to

predict whether the resulting complex will be neutral or charged is limited.⁴⁶ Indeed, half of the ΔpK_a values reported herein fall into the range of $0 < \Delta pK_a < 3$. How can one identify whether 7–19 are cocrystals or salts, especially where the FT-IR spectra may not provide adequate information?

The ΔpK_a values of cocrystals 1–6 were used as a reference to determine whether 7–19 are cocrystals or salts. As shown in Table 1, 4 possesses the largest value of ΔpK_a at 1.21, and proton transfer was not observed between meloxicam and salicylic acid. Although the molecular arrangement of various coformers may have an influence to the electron distribution and protonation of meloxicam, with the single-crystal XRD data of 1–6, it is reasonable to assert that all coformers involved in this study with ΔpK_a close to or less than 1.21 would potentially produce a cocrystal rather than a salt with meloxicam.⁴⁷ Based on this, with the exception of 9, all crystal forms prepared in this study can be identified as meloxicam cocrystals (Table 2). However, 9 remained questionable, because maleic acid exhibits a ΔpK_a of 2.25. Further investigation into the FT-IR spectrum of 9 was performed to identify the position of the proton. The carbonyl group of maleic acid in 9 exhibits a distinct peak at 1716 cm^{-1} , indicating that the carboxylic acid group is neutral rather than negatively charged.⁴⁸ Therefore, proton transfer does not occur between meloxicam and maleic acid, and 9 is a cocrystal of meloxicam and maleic acid.

4. Conclusions

Considering the enormous impact of pharmaceutical cocrystals upon crystal form diversity and the resulting opportunity to customize the physicochemical properties of APIs, it is unlikely that the relevance of crystal forms to drug delivery, intellectual property, and regulatory control will diminish in the near future. The science of crystal form selection will continue to evolve. In this context, meloxicam was selected as a case study to demonstrate how coformers can generate pharmaceutical cocrystals with the potential to improve the pharmacokinetic properties and the onset-of-action of the API. The supramolecular synthon approach afforded 19 cocrystals with pharmaceutically acceptable or toxicologically qualified carboxylic acids.

The use of multiple preparative techniques for almost all meloxicam cocrystals in this study would indicate that large-scale manufacturing of those cocrystals would be feasible should one of these cocrystals exhibit desired pharmacological properties. Among the 19 cocrystals reported herein, crystal structures of six (1–6) were determined. A salient feature in 1–6 is the two-point recognition carboxylic acid–azole/NH supramolecular heterosynthon. A prominent aspect of 1–3, 5, and 6 is the presence of the meloxicam dimer. The meloxicam molecules in 4, however, are juxtaposed such that the meloxicam dimer is absent. As part of the continuous crystal form selection process, all meloxicam cocrystals obtained in this study will be tested further via dissolution studies and *in vivo* pharmacokinetic studies.

Acknowledgment. We thank Mr. Raymond K. Houck for stimulating discussions and valuable input to the project.

Supporting Information Available: Additional characterization of the meloxicam cocrystals reported herein and crystal structure data in CIF format. This material is available free of charge via the Internet at <http://pubs.acs.org>.

References

- (1) Allen, L. V.; Popovich, N. G.; Ansel, H. C., *Ansel's pharmaceutical dosage forms and drug delivery systems*; Lippincott Williams and Wilkins: Baltimore, MD, 2005.
- (2) Byrn, S. R.; Pfeiffer, R. R.; Stephenson, G.; Grant, D. J. W.; Gleason, W. B. *Chem. Mater.* **1994**, *6*, 1148. Halebian, J. K. *J. Pharm. Sci.* **1975**, *64*, 1269.
- (3) Berge, S. M.; Bighley, L. D.; Monkhouse, D. C. *J. Pharm. Sci.* **1977**, *66*, 1.
- (4) Dublin, C. H. *Drug Delivery Technol.* **2006**, *6*, 34.
- (5) Khankari, R. K.; Grant, D. J. W. *Thermochim. Acta* **1995**, *248*, 61.
- (6) Vipagunta, S. R.; Brittain, H. G.; Grant, D. J. W. *Adv. Drug Delivery Rev.* **2001**, *48*, 3.
- (7) Zaworotko, M.; Arora, K. Pharmaceutical co-crystals: A new opportunity in pharmaceutical science for a long-known but little studied class of compounds. In *Polymorphism in Pharmaceutical Solids*, 2nd ed.; Brittain, H. G., Ed.; Informa Healthcare: London, 2009.
- (8) (a) Aaltonen, J.; Allesio, M.; Mirza, S.; Koradia, V.; Gordon, K. C.; Rantanen, J. *Eur. J. Pharm. Biopharm.* **2009**, *71*, 23. (b) Yin, S. X.; Grosso, J. A. *Curr. Opin. Drug Discovery Dev.* **2008**, *11*, 771.
- (9) Cheney, M. L.; Shan, N.; Healey, E. R.; Hanna, M.; Wojtas, L.; Zaworotko, M. J.; Sava, V.; Song, S.; Sanchez-Ramos, J. R. *Cryst. Growth Des.* **2010**, *10*, 394.
- (10) Desiraju, G. R. *Angew. Chem., Int. Ed. Engl.* **1995**, *34*, 2311.
- (11) (a) Pepinsky, R. *Phys. Rev.* **1955**, *100*, 971. (b) Desiraju, G. R., *Crystal Engineering: The Design of Organic Solids*; Elsevier: Amsterdam, 1989. (i) Schmidt, G. M. J. *Pure Appl. Chem.* **1971**, *27*, 647. (c) Shan, N.; Batchelor, E.; Jones, W. *Tetrahedron Lett.* **2002**, *43*, 8721. (d) Shan, N.; Bond, A. D.; Jones, W. *Cryst. Eng.* **2002**, *5*, 9. (e) Shan, N.; Bond, A. D.; Jones, W. *Tetrahedron Lett.* **2002**, *43*, 3101. (f) Shan, N.; Jones, W. *Tetrahedron Lett.* **2003**, *44*, 3687. (g) Bis, J. A.; Vishweshwar, P.; Weyna, D.; Zaworotko, M. J. *Mol. Pharmaceutics* **2007**, *4*, 401. (h) Shattock, T. R.; Arora, K. K.; Vishweshwar, P.; Zaworotko, M. J. *Cryst. Growth Des.* **2008**, *8*, 4533.
- (12) Allen, F. H. *Acta Crystallogr.* **2002**, *B58*, 380.
- (13) Almarsson, Ö.; Zaworotko, M. J. *Chem. Commun.* **2004**, 1889.
- (14) Shan, N.; Zaworotko, M. J. *Drug Discovery Today* **2008**, *13*, 440.
- (15) (a) Childs, S. L.; Chyall, L. J.; Dunlap, J. T.; Smolenskaya, V. N.; Stahly, B. C.; Stahly, G. P. *J. Am. Chem. Soc.* **2004**, *126*, 13335. (b) Banerjee, R.; Bhatt, P. M.; Ravindra, N. V.; Desiraju, G. R. *Cryst. Growth Des.* **2005**, *5*, 2299.
- (16) Good, D. J.; Rodriguez-Hornedo, N. *Cryst. Growth Des.* **2009**, *9*, 2252.
- (17) Karki, S.; Friscic, T.; Fabian, L.; Laity, P. R.; Day, G. M.; Jones, W. *Adv. Mater.* **2009**, *21*, 3905.
- (18) (a) Shan, N.; Toda, F.; Jones, W. *Chem. Commun.* **2002**, 2372. (b) Weyna, D. R.; Shattock, T.; Vishweshwar, P.; Zaworotko, M. J. *Cryst. Growth Des.* **2009**, *9*, 1106.
- (19) (a) Friščić, T.; Childs, S. L.; Rizvi, S. A. A.; Jones, W. *CrystEngComm* **2009**, *11*, 418. (b) Lu, E.; Rodriguez-Hornedo, N.; Suryanarayanan, R. *CrystEngComm* **2008**, *10*, 665.
- (20) (a) Remenar, J. F.; Morissette, S. L.; Peterson, M. L.; Moulton, B.; MacPhee, J. M.; Guzman, H. R.; Almarsson, O. *J. Am. Chem. Soc.* **2003**, *125*, 8456. (b) Basavoji, S.; Bostrom, D.; Velaga, S. P. *Cryst. Growth Des.* **2006**, *6*, 2699. (c) Chen, A. M.; Ellison, M. E.; Peresypkin, A.; Wenslow, R. M.; Variankaval, N.; Savarin, C. G.; Natishan, T. K.; Mathre, D. J.; Dormer, P. G.; Euler, D. H.; Ball, R. G.; Ye, Z. X.; Wang, Y. L.; Santos, I. *Chem. Commun.* **2007**, 419. (d) Remenar, J. F.; Peterson, M. L.; Stephens, P. W.; Zhang, Z.; Zimenkov, Y.; Hickey, M. B. *Mol. Pharmaceutics* **2007**, *4*, 386. (e) Zegarac, M.; Mestrovic, E.; Dumbovic, A.; Devic, M.; Tudja, P. Pharmaceutically Acceptable Co-Crystalline Forms of Sildenafil, WO 2007/080362 A1, 2007. (f) Childs, S. L.; Rodriguez-Hornedo, N.; Reddy, L. S.; Jayasankar, A.; Maheshwari, C.; McCausland, L.; Shipplett, R.; Stahly, B. C. *CrystEngComm* **2008**, *10*, 856. (g) Shiraki, K.; Takata, N.; Takano, R.; Hayashi, Y.; Terada, K. *Pharm. Res.* **2008**, *25*, 2581. (h) Stanton, M. K.; Bak, A. *Cryst. Growth Des.* **2008**, *8*, 3856. (i) Stanton, M. K.; Tufekci, S.; Morgan, C.; Bak, A. *Cryst. Growth Des.* **2009**, *9*, 1344. (j) Trask, A. V.; Motherwell, W. D. S.; Jones, W. *Cryst. Growth Des.* **2005**, *5*, 1013.
- (21) Ahmed, M.; Khanna, D.; Furst, D. E. *Exp. Opin.* **2005**, *1*, 739.
- (22) (a) Thompson, J. P.; Sharpe, P.; Kiani, S.; Owen-Smith, O. *Br. J. Anaesth.* **2000**, *84*, 151. (b) Roughan, J. V.; Flecknell, P. A. *Eur. J. Pain* **2003**, *7*, 397.
- (23) Engelhardt, G.; Homma, D.; Schlegel, K.; Utzmann, R.; Schnitzler, C. *Inflammation Res.* **1995**, *44*, 423.

- (24) (a) Stei, P.; Kruss, B.; Wiegler, J.; Trach, V. *Br. J. Rheumatol.* **1996**, 35 (Suppl. 1), 44. (b) Lehmann, H. A.; Baumeister, M.; Luetzen, L.; Wiegler, J. *Inflammopharmacology* **1996**, 4, 105.
- (25) (a) Burdan, F. *Toxicology* **2005**, 211, 12. (b) Harirforoosh, S.; Aghazadeh-Habashi, A.; Jamali, F. *Clin. Exp. Pharmacol. Physiol.* **2006**, 33, 917.
- (26) Seedher, N.; Bhatia, S. *AAPS PharmSciTech* **2003**, 4, No. 33.
- (27) Takagi, T.; Ramachandran, C.; Bermejo, M.; Yamashita, S.; Yu, L. X.; Amidon, G. L. *Mol. Pharmaceutics* **2006**, 3, 631.
- (28) Luger, P.; Daneck, K.; Engel, W.; Trummlitz, G.; Wagner, K. *Eur. J. Pharm. Sci.* **1996**, 4, 175.
- (29) Coppi, L.; Sanmarti, M. B.; Clavo, M. C. Crystalline Forms of Meloxicam and Processes for Thier Preparation and Interconversion, US Patent 6,967,248 B2, 2005.
- (30) Davies, N. M.; Skjodt, N. M. *Clin. Pharmacokinet.* **1999**, 36, 115.
- (31) Ghorab, M. M.; Abdel-Salam, H. M.; El-Sayad, M. A.; Mekhel, M. M. *AAPS PharmSciTech* **2004**, 5, No. 59.
- (32) Han, H. K.; Choi, H. K. *Eur. J. Pharm. Biopharm.* **2007**, 65, 99.
- (33) Defazio, S.; Cini, R. *J. Chem. Soc., Dalton Trans.* **2002**, 1888.
- (34) (a) Bock, T.; Saegmueller, P.; Sieger, P.; Tuerck, D. Meloxicam for Oral Administration, US Patent 6,869,948 B1, 2005. (b) Struengmann, A.; Freudensprung, B.; Klokke, K. New Pharmaceutical Compositions of Meloxicam with Improved Solubility and Bioavailability, International Patent WO 99/09988 A1, 1999.
- (35) Meloxicam for this study was purchased as form I, which was stable at ambient conditions throughout the study.
- (36) Myz, S. A.; Shakhshneider, T. P.; Fucke, K.; Fedotov, A. P.; Boldyreva, E. V.; Boldyrev, V. V.; Kuleshova, N. I. *Mendeleev Commun.* **2009**, 19, 272.
- (37) Childs, S. L.; Hardcastle, K. I. *Cryst. Growth Des.* **2007**, 7, 1291.
- (38) Bruker SMART, SAINT-Plus, SADABS, XP and SHELXTL; Bruker: Madison, WI, 1997.
- (39) Sheldrick, G. M. *SHELXTL*, University of Göttingen: Göttingen, Germany, 1997.
- (40) It must be noted that the CSD structures have not been systematically populated to provide a balanced representation of the various functional groups. Although the supramolecular synthon approach has been successfully used in the various pharmaceutical cocrystal studies, the CSD statistical result here could be biased.
- (41) Fabiola, G. F.; Patabhi, V.; Manjunatha, S. G.; Rao, G. V.; Nagarajan, K. *Acta Crystallogr.* **1998**, C54, 2001.
- (42) CSD version 5.31, November 2009 release including May 2010 update. Search parameters: organics only, 3D coordinates determined, $R < 7.5\%$.
- (43) Etter, M. C. *Acc. Chem. Res.* **1990**, 23, 120.
- (44) Ki, H. M.; Choi, H. K. *Arch. Pharm. Res.* **2007**, 30, 215.
- (45) (a) Stahl, P. H.; Wermuth, C. G., *Handbook of Pharmaceutical Salts: Properties, Selection, and Use*; WILEY-VCH: Zurich, 2002. (b) Bhogala, B. R.; Basavoju, S.; Nangia, A. *CrystEngComm* **2005**, 7, 551. (c) Delori, A.; Suresh, E.; Pedireddi, V. R. *Chem.—Eur. J.* **2008**, 14, 6967.
- (46) Childs, S. L.; Stahly, G. P.; Park, A. *Mol. Pharmaceutics* **2007**, 4, 323.
- (47) Identification of cocrystals based on ΔpK_a values is straightforward but also could be less rigorous. However, confirmation of relevant proton locations in **8**, **9**, and **11–20** remains inconclusive using available characterization techniques. As part of the continuous study, further attempts of single-crystal XRD characterization for **8**, **9**, and **11–20** are being undertaken.
- (48) Silverstein, R. M.; Webster, F. X.; Kiemle, D. J. *Spectroscopic Identification of Organic Compounds*; John Wiley & Sons: New York, 2005.
- (49) (a) pK_a Data, http://research.chem.psu.edu/brpgroup/pKa_compilation.pdf. (b) Minnick, L. J.; Kilpatrick, M. *J. Phys. Chem.* **1939**, 43, 259.
- (50) (a) Chemical Dictionary Online, 1-Hydroxy-2-naphthoic acid. http://www.chemicaldictionary.org/dic/1/1-Hydroxy-2-naphthoic-acid_919.html (August 2009); (b) Brittain, H. G.; Prankerd, R. J. *Profiles of drug substances, excipients, and related methodology*; Academic Press: New York, 2007; p 369; (c) Cabelli, D. E.; Bielski, B. H. J. *Z. Naturforsch., B* **1985**, 40, 1731.
- (51) (a) Erdemgil, F. Z.; Sanli, S.; Sanli, N.; Özkan, G.; Barbosa, J.; Guiteras, J.; Beltrán, J. L. *Talanta* **2007**, 72, 489. (b) Castro, J. L.; Ramírez, M. R. L.; Tocón, I. L.; Otero, J. C. *J. Raman Spectrosc.* **2002**, 33, 455.